International Journal of Industrial Electronics, Control and Optimization © 2018 IECO

Vol. 1, No. 2, pp. 103-113, September (2018)

Control Structure Design and Dynamic Modeling for Atmospheric Distillation Column: Effect of Increase Capacity

Mir Mohammad Khalilipour,[a] **Farhad Shahraki**,[b] **Jafar Sadeghi**,[c] and **Kiyanoosh Razzaghi**[d]

ABSTRACT

The paper presents the computer simulation of a multivariate control algorithm. Industrial relevance is given as the problem is derived from a real plant, an industrial atmospheric distillation column at Shiraz refinery. The control performance of the industrial column using relative gain array (RGA) and relative normalized gain array (RNGA) configurations has been examined for nominal operating capacity and 10% increase in capacity. The results show that RNGA structure remains stable and has an acceptable control performance for both nominal and increased capacity. RGA structure unlike RNGA changes at the increased capacity and has some difficulties in crude oil switch scenario. It has also been shown that the furnace duty will increase considerably in the case of using RGA for operating at increased capacity. The results indicate that RNGA represents better decision for loop pairing and control structure selection and can solve control issues of industrial distillation column specifically for uncertain feed condition.

ARTICLE INFO

Keywords:
Control Configuration
Dynamic Simulation
RGA
RNGA
Uncertain Feed Condition
Article history:
Received March. 13, 2018
Accepted July. 8, 2018

I. INTRODUCTION

The atmospheric distillation column, known as atmospheric pipestills (AP), is at the heart of any crude distillation units (CDU) in the oil refineries. The separation process like AP always encounters with complexities, nonlinearity and long time delays. There is a strong motivation between academia and industrial specialists to deal with operability and control performance of complex unit issues during the past two decades[1]. From a process control point of view, any significant change in the AP feed due to any reason should be considered precisely. However, because of the ill-conditioned nature of APs, maintaining the process at the optimal operating conditions is a sophisticated task. Finding the best control structure through input and output variables is strongly related to crude oil properties and unit conditions[2]. Increasing feed rate by company policies or retrofit and optimization cannot be directly applied to the actual system since the concept of control performance is ignored. Nevertheless, usually the control performance of the optimized process has not been considered. Growing interest in capacity increase of APs has raised challenges on control performance of the process. In the APs the highest quality of production as well as lower operating cost could be achieved by selecting the best control structure[3].

Control configuration selection has been considered by several authors[4–10], but there is no a general agreement among the authors about the best configuration. The main works for selection of manipulated/controlled variables pairings have focused upon using interaction measures, such as relative gain array[11]. The RGA is a steady-state measure of interactions for decentralized control and has been addressed by many authors[6,12–14]. Skogestad et al.[6] proposed frequency-dependent RGA is useful for selecting appropriate control configuration in distillation columns. Several studies on the control structure selection of industrial plant specifically focusing on RGA method have been presented in the recent paper[15–17]. Loop pairing decision based on only steady state gain matrix and without considering dynamic information process may lead to improper interaction measures and consequently incorrect control configuration. The problem motivated researchers to utilize dynamic RGA (DRGA), which considers effect of process dynamics. Mc Avoy et al.[18] proposed transfer function model instead of RGA. Relative effective gain array (REGA), the combination of RGA and DRGA are investigated by Xiong et al.[19]. Relative normalized gain array (RNGA) introduced by He et al.[20] for loop interaction measures. They reported RNGA makes more comprehensive description for loop interaction and provides the best pairing among other

[a] Corresponding Author: a.khalilipour@eng.usb.ac.ir, Tel: +98-54-3113-2813, Fax: +98-54-33447092, Center for process Integration and Control, Department of Chemical Engineering, University of Sistan and Baluchestan, Zahedan, Iran
[b] Center for process Integration and Control, Department of chemical Engineering, University of Sistan and Baluchestan, Zahedan, Iran
[c] Center for Process Integration and Control, Department of chemical Engineering, University of Sistan and Baluchestan, Zahedan, Iran
[d] Center for Process Integration and Control, Department of chemical Engineering, University of Sistan and Baluchestan, Zahedan, Iran
http://dx.doi.org/10.22111/ieco.2018.23895.1023

methods (i.e. RGA, DRGA and REGA).

This paper addresses the selection of control structure and dynamic modeling for an industrial atmospheric distillation column using the RNGA and RGA methods. An industrial AP modeled and simulated using ASPEN software to present dynamic behavior of the column. The open loop tests between all potential manipulated/controlled variables were examined to identify process gain, dead time and time constant. The RGA and RNGA have been utilized to select proper loop pairings in the case of MIMO system of AP. Dynamic simulation was linked to MATLAB in order to consider the control performance of the column for both RGA and RNGA configurations at the current and increased capacity of the unit. The paper focuses on the practical interesting based on the real world data. The main contribution of the current study are as follows:

1. Dynamic behavior of an industrial crude distillation column based on real world data has been investigated while previous works on pairing selection was tested on the unrealistic column.
2. RGA and RNGA pairing methods have not been investigated on the industrial crude oil column using the dynamic measurements as well as perfect manipulators.
3. The new control structure (for nominal and increased capacity) has good control performance and succeed to solve the control problem of industrial unit.
4. Inferential Aspen soft sensors was utilized to monitor the ASTM temperature instead of industrial conventional method.

II. PROCESS MODEL SIMULATION

The conventional measurement method to describe product quality in crude distillation is cut point which is time consuming and ponderous procedure. Therefore, in crude distillation process the fraction quality is usually represented by ASTM standard method[21].

In this approach the 5% of ASTM affect the lighter components while, the 95% of ASTM affect the heavy components. It is a sophisticated job to relate the ASTM to product quality directly in the real plants. Using the soft sensors to online estimation of desired product properties is the only approach to control product quality precisely[22]. In this study, soft sensors are applied to monitor the ASTMD86 temperature of naphtha, kerosene and gas oil. The schematic diagram of industrial AP at the Shiraz refinery depicts in Fig. 1a. The column has three side strippers which the quality of the side stream products specify by ASTM soft sensors. Further information about case study can be found in the appendix A.

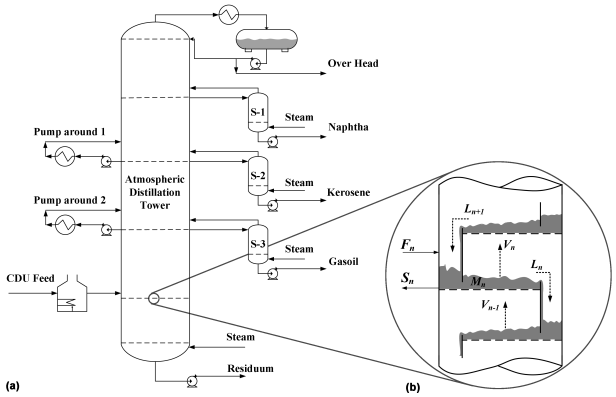


FIG. 1. **(a)** Schematic of the atmospheric crude oil distillation column, **(b)** Streams in the nth stage of distillation column.

The crude oil composed of complex hydrocarbon mixtures. The standard approach was applied to lump feed into smaller number of pseudo-component in order to simulate the process[23]. In this study, 38 pseudo-components were considered and characterized by boiling point, API and molecular weight. In the process simulation, it is a common practice to make some reasonable assumption to simplify the simulation:

1. Ideal stage for each tray was assumed.
2. The efficiency of the tower and pressure drop between trays were assumed to be constant.
3. Since composition of the mixture varies slightly, heat capacity of products can also be assumed to be constant within the range of AP operation.
4. All the water flows enter to the column can be assumed to be completely in the vapor phase.

Consider a stage n on the distillation column as shown in Fig. 1b. The overall mass balance for stage n can be expressed as:

$$\frac{dM_n}{dt} = L_{n+1} + V_{n-1} + F_n - L_n - V_n - S_n \quad (1)$$

Component mass balance for stage n is expresses by:

$$\begin{aligned}\frac{d(M_n x_{n,j})}{dt} =& L_{n+1}x_{n+1,j} + V_{n-1}y_{n-1,j} + F_n z_{n,j} \\ & - L_n x_{n,j} - V_n y_{n,j} - S_n x_{n,j}\end{aligned} \quad (2)$$

The Brown K10 (BK10) model is used for real components as well as pseudo-components. This method is strictly applicable for medium to heavy hydrocarbons at low pressures[24].

Steady-state and dynamic simulation has been carried out using Aspen Plus and Aspen dynamic, respectively. The result of Aspen Dynamic soft sensors for ASTM-D86 boiling point and the oil lab data are compared in Fig 2. Figs. 2a-c indicate the ASTM-D86 temperature for naphtha, kerosene and gas oil, respectively. Fig. 2 illustrates

that the simulation results are in a good agreement with real industrial data. Based on the simulation result and lab data the root mean square error RMSE for the side products are 1%, 2% and 1% for naphtha, kerosene and gas oil, respectively.

The simulation was carried out for the nominal operational condition and 10% increase in capacity of the column. To obtain good results that can be utilized in a real control system, it is important to accurately model the loop dynamics. In this study, for dynamic simulation the conventional PI controller is implemented. The PI controller is relatively simple to tune and the maintenance cost is low. The controller is tuned by Tyreus-Luyben method[25] to achieve robust performance. The method is less aggressive than Ziegler-Nichols with lower gain and larger integral times. The following measurement-delay was used in control loops:

1. For overhead temperature control loop, a 1-min deadtime was assumed.
2. For the furnace temperature loop and quality control loops, 3-min deadtime was considered.

The dead time values are usually selected practically. Since the dynamics of a fired furnace is usually slower than other temperature loops in distillation column 3-min deadtime for furnace control loop was utilized instead of normal 1-min deadtime. Further information can be find in earlier publication[26]. Relay feedback test was run between inputs and outputs on all controllers for all selected control configurations. A sequential tuning procedure was used to obtain ultimate gain and period. Then the control parameters estimated by the method proposed by Tyreus and Luyben[25].

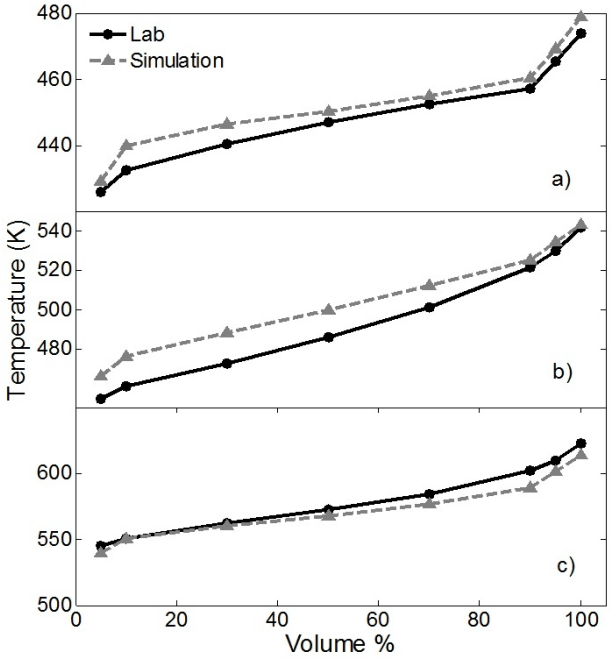


FIG. 2. ASTM-D86 for simulation and oil lab data, **(a)** naphtha, **(b)** kerosene, **(c)** gas oil.

TABLE I. Input variables

Variable	Description	Unit
u_1	Side-draw of naphtha	kg/h
u_2	Side-draw of kerosene	kg/h
u_3	Side-draw of gas oil	kg/h
u_4	Furnace duty	kW
u_5	Reflux split fraction	–
u_6	Heat removed in pumparound1	kW
u_7	Heat removed in pumparound2	kW

III. CONTROL STRUCTURE SELECTION

Control structure selection method pairs the best controlled/manipulated variables to reach optimum point of operation. The main controlling goal of the distillation process is to maintain the product quality within the specified range. Levels and pressures should be controlled as primary control objective. This is the simplistic approach to reduce the alternative options of the control configuration problem.

Basic controllers in closed loop system are including top pressure of main column, pressure of strippers, reflux-drum level and base level of the column and strippers. In this study, the input variables after obviating pressure and level control loops are heat removal from mid-tower condensers, furnace duty, reflux split fraction and side draw flow rate of strippers, while the output variables are overhead temperature and true boiling point (95% ASTMD86) of naphtha, kerosene and gas oil. The side stripper steam were fixed by setting ratio controller between side product flowrate and superheating steam of strippers. Since overhead stream consists of two products, inferential temperature control was applied to control both quality of liquid (light naphtha) and gas products. Manipulated and controlled variables are given in Tables I and II, respectively. There are 7 manipulated and 4 controlled variables which indicate a 7×4 multi-input multi-output (MIMO) control system. The next step is to select the proper manipulated/controlled variables parings. The transfer function matrix $\mathbf{G}$ is described as:

$$\mathbf{G(s)} = [g_{ij}(s)]_{n\times n} \tag{3}$$

TABLE II. Output variables

Variable	Description	Set point	Unit
y_1	Overhead temperature	420	K
y_2	95% -ASTMD86 of naphtha	470	K
y_3	95% -ASTMD86 of kerosene	535	K
y_4	95% -ASTMD86 of gas oil	601	K

$$g_{ij}(s) = \frac{k_{ij}e^{-\theta_{ij}s}}{\tau_{ij}s+1} \tag{4}$$

where, the τ_{ij} is time constant and θ_{ij} is dead time of transfer function. The gain matrix of transfer functions can be express as:

$$\mathbf{K} = [k_{ij}]_{n\times n} \tag{5}$$

The RGA for the square transfer function matrix $\mathbf{G}$ is defined as:

$$\mathbf{\Lambda} = \mathbf{K} \times \left(\mathbf{K}^{-1}\right)^T \tag{6a}$$

$$\mathbf{\Lambda} = [\lambda_{ij}]_{n\times n} = \frac{k_{ij}}{\widehat{k}_{ij}} \tag{6b}$$

where, the operation $\times$ denotes element by element multiplication and $\hat{K}_{ij}$ is the gain between output variable y_i and input variable u_j when all other loops are closed. Interpretation on how RGA influences pairing of manipulated with controlled variables is related to the sign and value of λ_{ij}. The objective is to pair the controlled and manipulated variables while the relative gain parameter (λ_{ij}) is positive and close to one as possible. Normalized gain matrix can be described as:

$$\mathbf{K}_N = [k_{N,ij}]_{n\times n} \tag{7}$$

$$k_{N,ij} = \frac{k_{ij}}{\tau_{\mathrm{ar},ij}} = \frac{k_{ij}}{\tau_{ij}+\theta_{ij}} \tag{8}$$

where, $k_{N,ij}$ is the normalized gain of $g_{ij}(s)$ and τ_{ar} is the average residence time. Relative normalize gain (RNG) can be obtain by substituting $\mathbf{K}_N$ with steady state gain in the relative gain (RG). The RNGA matrix is described as:

$$\mathbf{\Phi} = \mathbf{K}_N \times \left(\mathbf{K}_N^{-1}\right)^T \tag{9a}$$

$$\mathbf{\Phi} = [\phi_{ij}]_{n\times n} = \frac{k_{N,ij}}{\widehat{k}_{N,ij}} \tag{9b}$$

where, $\hat{k}_{N,ij}$ is the effective gain between output variable y_i and input variable u_j when all other loops are closed. The goal is similar to RGA is the relative normalize gain parameter (ϕ_{ij}) is positive and close to one as possible. The advantage of using RNGA is considering dynamic information to calculate loop interaction instead of utilizing only steady state gain. RNGA is controller-type independent and also uses the average residence time, which requires much less calculation in comparison to DRGA and REGA[20].

The RGA and RNGA method is only applicable to square gain matrix. For the case the gain matrix is non-square, the squaring down process can be used to extract all square subsystems[4]. In the squaring down approach, 35 matrices ($C_4^7 = 35$) were extracted. The RGA and RNGA method was applied for all of 35 square gain and normalized gain matrices. The best structure among square RGA and RNGA matrices was obtained using the minimum value of condition number:

$$k(\mathbf{\Lambda}) = \frac{\sigma_{\max}(\mathbf{\Lambda})}{\sigma_{\min}(\mathbf{\Lambda})} \tag{10a}$$

$$k(\mathbf{\Phi}) = \frac{\sigma_{\max}(\mathbf{\Phi})}{\sigma_{\min}(\mathbf{\Phi})} \tag{10b}$$

All possible 4×7 process gain matrices identified for each capacity. The identified dynamic process information and the best pairing can be found in appendix B. According to Eq. (10b), the selected square matrices of RGA and RNGA have the minimum value of condition number. In the square matrices, values of λ_{ij} and ϕ_{ij}, that is positive and close to one as possible, are selected for pairing. Thereupon the selected structures provide best pairing of manipulated/controlled variables, which cope with the direct control and less interaction in system. It is observed that the proposed configurations of RGA and RNGA for the nominal capacity are different. The primary controllers as well as the control structure of RGA and RNGA depicts in Fig. 3 and Fig. 4, respectively. The superheating steam of main column and strippers are fixed by ratio controller, which is not shown in the figures in order to avoid flowsheet complexity. Fig. 3 shows that the RGA paring loops while Fig. 4 elucidates the RNGA pair loops. Bothe structure are almost the same except overhead temperature control loops. The RGA utilize the cascade control loop for overhead temperature as it shown in Fig. 3. Fig. 3 and 4 are also shown the primary controller of the AP column which are include pressure and temperature of the main and stripper vessels. The RGA and RNGA matrices recalculated using process transfer matrix (see Appendix B, Eq. (12)) for 10% increase in capacity. The calculation results show that the RNGA structure remains the same but the RGA configuration was changed.

IV. RESULTS AND DISCUSSIONS

Dynamic simulation is used to examine control performance and capability of disturbance rejection for selected structures.

Load rejection capability of the selected configuration by RGA and RNGA are tested by ±5% step change in the feed rate. Figs. 5 and 6 show the dynamic response of the column for RGA and RNGA structures, respectively, in which the column operates at the nominal capacity. The results show that both RGA and RNGA configurations in nominal capacity can fully reject the loads.

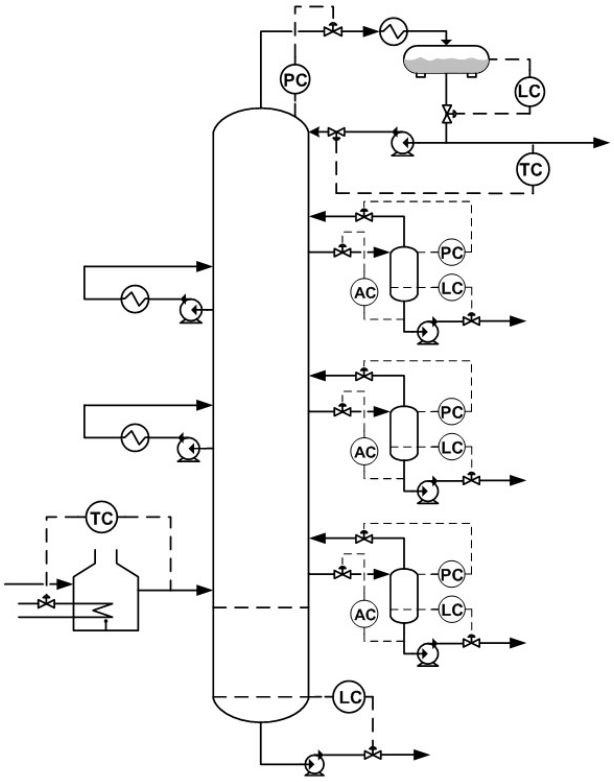


FIG. 3. Control configuration of RGA.

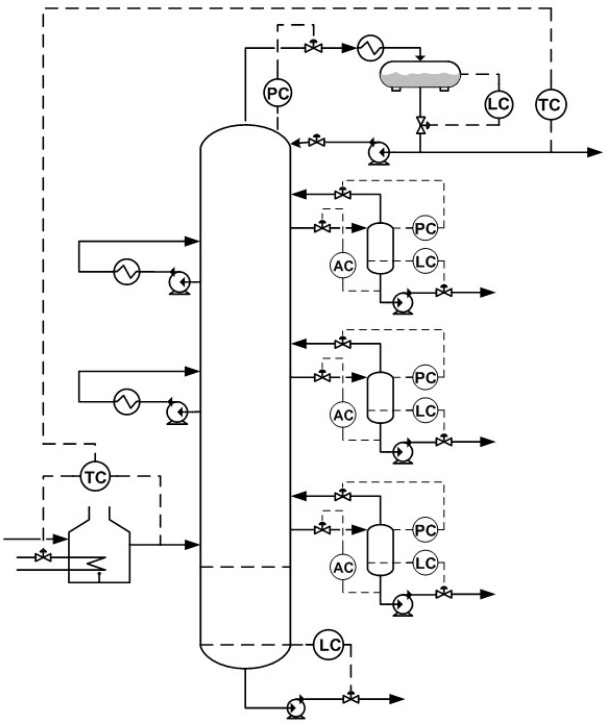


FIG. 4. Control configuration of RNGA.

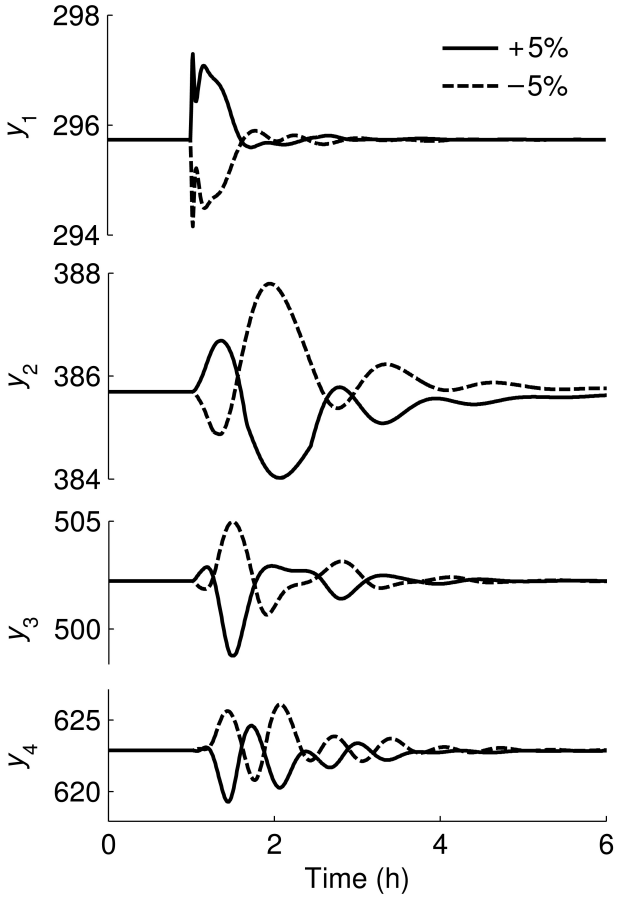


FIG. 5. Output response to ±5% step change in feed rate for RGA structure.

Dynamic response of control configurations for 10% increase in the capacity are illustrated in Fig. 7 for RGA and RNGA. The capacity increase starts at time 1 hour and the column capacity reaches to 10% increase within 5 hours. However, the RGA structure has a good control performance at the nominal capacity, but the dynamic responses of kerosene and naphtha quality become oscillatory near the upper limit of increased capacity. Fig. 7 illustrates that unlike the RGA configuration, RNGA has good performance in the case of capacity increase. The input change for capacity increase of the column is shown in Fig. 8. Fig. 8 reveals that the RGA structure utilizes furnace duty (u_4) more than RNGA structure. The results show that the column based on RGA structure will be utilized furnace duty about 5000 kW more than RNGA. The output responses of the column at the increased capacity were also examined by ±5% step change in the feed rate for RGA and RNGA separately. The results are shown in Fig. 9 and Fig. 10 for RNGA and RGA, respectively. Fig. 9 illustrates that the RNGA configuration has a good load rejection capability for the increased capacity. Fig. 10 elucidates that the RGA configuration has good control performance for 5% step change but the performance of +5% is not ac-

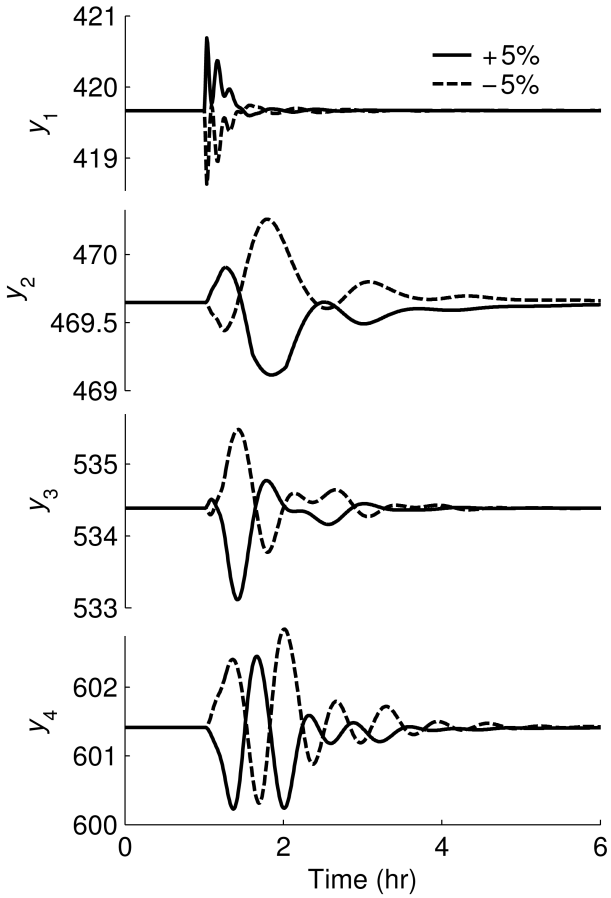


FIG. 6. Output response to ±5% step change in feed rate for RNGA structure.

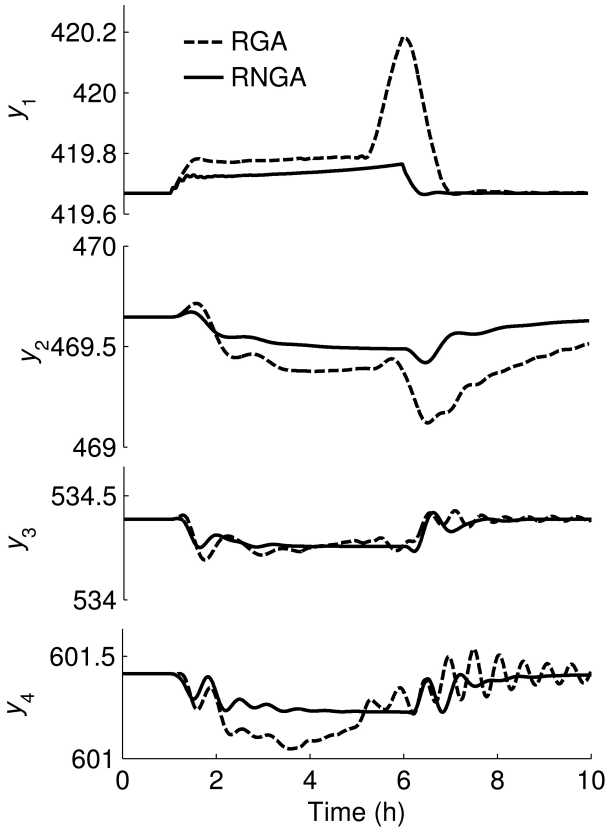


FIG. 7. Dynamic response for 10% increase in column capacity.

ceptable. The reason lies within the fact that when the capacity decreased by 5%, the control structure behavior is close to the control structure of the lower limit.

The Crude switches are the most important disturbance to crude units. For better consideration of control performance of the column were examined by crude oil switch at the increased capacities. In this case, the crude switch was applied to the column according to Table III. The switch crude oil was considered by blending the initial crude oil with light naphtha. Fig. 11 provides a comparison between RGA and RNGA performances for crude switch. The RNGA has acceptable performance to reject the crude switch disturbance. However, the naphtha side draw for RGA method was vanished to reject the disturbance, the controller has been failed to keep naphtha quality within its specification. However, the RGA configuration works properly at the nominal capacity of the process but because of considering only the steady state gain matrix, the configuration may lead to improper control performance. It is worthy to note that the loop pairing decision based on RNGA method presents more comprehensive description for loop interaction. The results overtly verify that the proposed configuration of RNGA has a good output control performance for regulatory problem at both of nominal and increased capacities. The advantage of RNGA compared with RGA provides better interaction measure and loop pairing decision that allows the control configuration works more properly at the feed condition uncertainty. Moreover, the results verify the investigation which was addressed by He et al.[20] and reveals that RNGA does not limited to unrealistic examples and has capability to use in industrial issues in order to solve control problem in real world application.

TABLE III. Output variables

Vol. % distilled	TBP for initial crude feed (K)	TBP for switched crude feed (K)
0	269	270
5	322	316
10	360	355
30	478	455
50	585	573
70	702	694
90	860	850
95	935	927
100	995	988

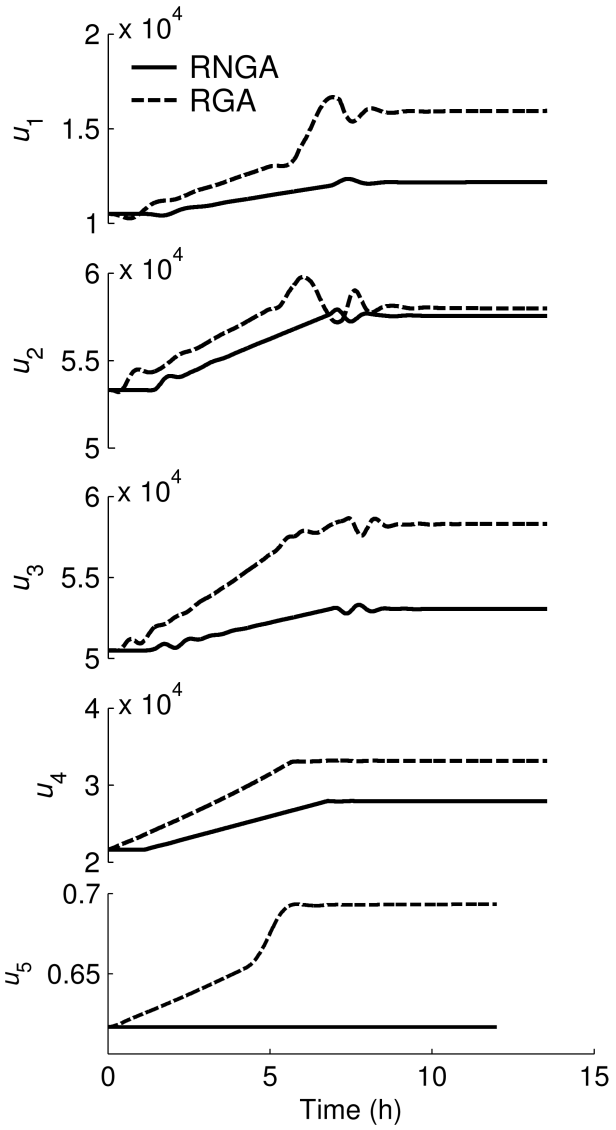


FIG. 8. Input changes for 10% increase in column capacity.

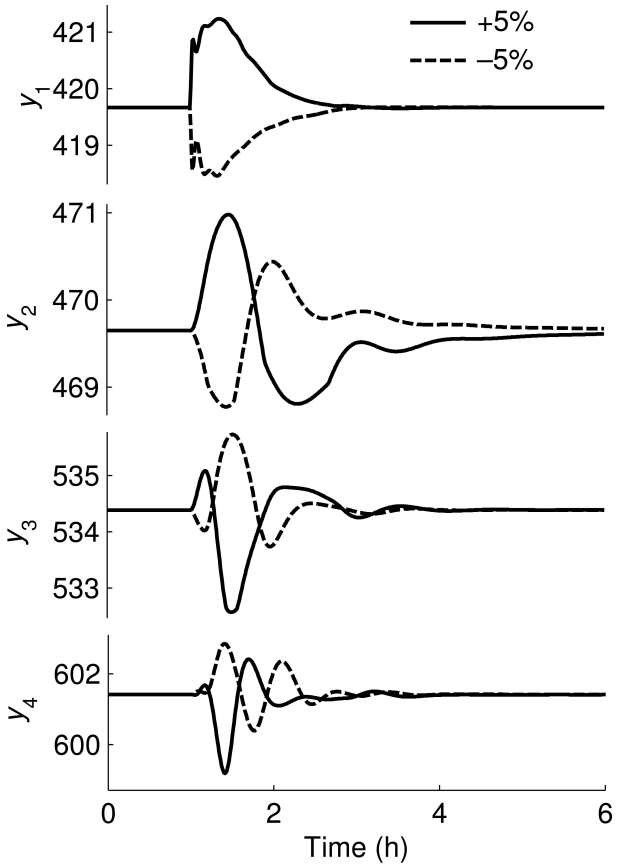


FIG. 9. Output response to ±5% step change in feed rate for RNGA structure.

V. CONCLUSIONS

The control configuration selection for industrial AP for nominal capacity and 10% capacity increase has been addressed based on the RGA and RNGA methods. Dynamic simulation is used to evaluate control performance and capability of disturbance rejection for both methods. The results show that the RNGA unlike the RGA structure will remain stable for current and increased capacity. However, RGA has been frequently used for control structure selection; the result show that only use of steady state gain cannot make a comprehensive decision for loop pairing. The main advantage of using RNGA for industrial column compared with RGA is that transient information is utilized to pair variables instead of steady state information. The result of comparison between RGA and RNGA correspond closely to those obtained by He et al. and Yunhui et al.[20,27]. It is important to highlight that the results present an acceptable control performance as well as energy efficient operation of AP in uncertain feed capacity. The proposed configuration of RNGA can solve the potential control problems of the column in the case of capacity increase and crude switch.

APPENDIX

A. Case study: Shiraz Refinery crude oil distillation column

The column used in this work is Atmospheric distillation tower of Shiraz Refinery. The column separates oil to various fractions such as overhead products, naphtha, kerosene and gas oil through complex and nonlinear process. The column includes 43 trays, two mid-tower condensers (pumparounds) and three 6-stage strippers. It operates at the nominal operating capacity of $8,750$ *cum/day*. Superheated stripping steam is injected from bottom of the main column and strippers. The steam adjusts temperature profile of the main column and removes any light hydrocarbon from the stripper's side product. The feed preheats by the first

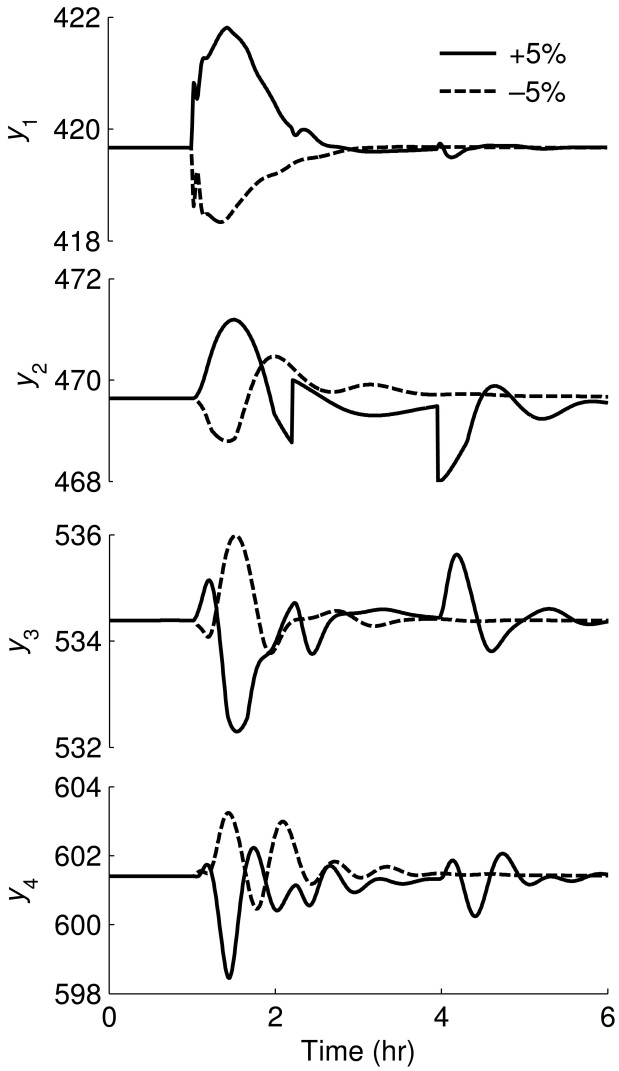


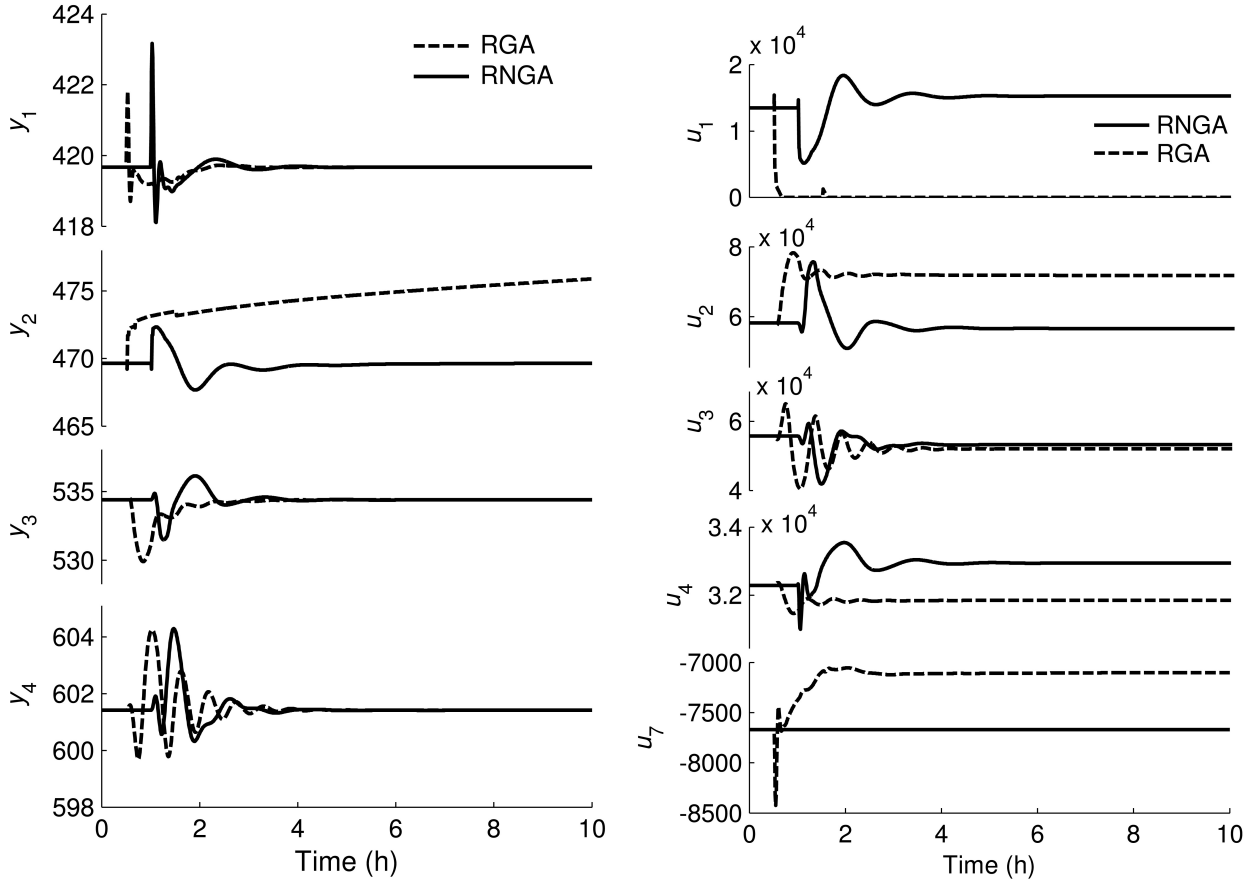
FIG. 10. Output responses to set point tracking for RGA configuration.

pumparound, kerosene and gas oil. The fired heater eventually causes feed temperature to rise to about $640K$.

B. Dynamic process information

Transfer function matrix for the nominal and increased capacity of distillation column are described by Eqs. (11) and (12), respectively: The best control structure based on Eq. (10b) among 35 square matrices (4×4) for RGA and RNGA according to Eqs. (6b) and (9b) in the nominal operating capacity obtained as the Eqs. (13) and (14). The selected configuration of RGA and RNGA for 10% increase in capacity obtained as the Eqs. (15) and (16). In these matrices the best pairing indicated by underline between input and output variables.

$$
\begin{array}{c} \\ y_1 \\ y_2 \\ y_3 \\ y_4 \end{array}
\begin{array}{c}
\begin{array}{ccccccc} u_1 & u_2 & u_3 & u_4 & u_5 & u_6 & u_7 \end{array} \\
\left(\begin{array}{ccccccc}
\frac{-(1.5\times10^{-5})e^{-10s}}{3.5s+1} & \frac{-(1.2\times10^{-5})e^{-12s}}{0.5s+1} & \frac{-(5\times10^{-5})e^{-5s}}{10s+1} & \frac{0.7e^{-1.5s}}{12s+1} & \frac{-305e^{-0.6s}}{2s+1} & \frac{(1.4\times10^{-6})e^{-s}}{2.5s+1} & \frac{(2\times10^{-6})e^{-s}}{3.5s+1} \\
\frac{0.0007e^{-9s}}{73s+1} & \frac{(4\times10^{-7})e^{-4s}}{10s+1} & \frac{-0.0001e^{-12s}}{68s+1} & \frac{0.88e^{-6s}}{49s+1} & \frac{-510e^{-30s}}{93s+1} & \frac{(2.1\times10^{-6})e^{-4s}}{63s+1} & \frac{(1.9\times10^{-6})e^{-4.5s}}{61s+1} \\
\frac{0.002e^{-5s}}{44s+1} & \frac{0.001e^{-4s}}{29s+1} & \frac{-(3\times10^{-5})e^{-9s}}{10s+1} & \frac{0.75e^{-5s}}{21s+1} & \frac{-516e^{-5s}}{31s+1} & \frac{(2.7\times10^{-6})e^{-3s}}{22s+1} & \frac{(3.35\times10^{-6})e^{-4s}}{16.5s+1} \\
\frac{0.0017e^{-6.5s}}{39.5s+1} & \frac{0.0014e^{-15s}}{36s+1} & \frac{0.0011e^{-18s}}{29s+1} & \frac{0.37e^{-25s}}{4.5s+1} & \frac{-569e^{-8s}}{31s+1} & \frac{(2.6\times10^{-6})e^{-5s}}{20.5s+1} & \frac{(3.1\times10^{-6})e^{-4s}}{13.5s+1}
\end{array} \right)
\end{array}
\tag{11}
$$



(a) Output response

(b) Input changes

FIG. 11. Crude switch performance for RGA and RNGA structure.

$$\begin{array}{c} \\ y_1 \\ y_2 \\ y_3 \\ y_4 \end{array} \begin{array}{c} \begin{array}{ccccccc} u_1 & u_2 & u_3 & u_4 & u_5 & u_6 & u_7 \end{array} \\ \begin{pmatrix} \frac{-(9.8\times10^{-6})e^{-10s}}{2s+1} & \frac{-(1.9\times10^{-6})e^{-s}}{0.4s+1} & \frac{-(4.7\times10^{-5})e^{-4.5s}}{10s+1} & \frac{1.02e^{-1.5s}}{23s+1} & \frac{-318e^{-0.6s}}{2s+1} & \frac{(1.3\times10^{-6})e^{-0.7s}}{2.5s+1} & \frac{(1.35\times10^{-6})e^{-s}}{3.5s+1} \\ \frac{0.001e^{-8s}}{63s+1} & \frac{(2.7\times10^{-5})e^{-5s}}{15s+1} & \frac{-0.0001e^{-11s}}{64s+1} & \frac{1.41e^{-22s}}{50s+1} & \frac{-513e^{-4s}}{72s+1} & \frac{(1.9\times10^{-6})e^{-3.5s}}{54s+1} & \frac{(2.5\times10^{-6})e^{-4s}}{48s+1} \\ \frac{0.0017e^{-4.5s}}{40s+1} & \frac{0.0009e^{-4s}}{26s+1} & \frac{-(4\times10^{-5})e^{-8s}}{11s+1} & \frac{1.07e^{-5.5s}}{35s+1} & \frac{-517e^{-5s}}{29s+1} & \frac{(2.46\times10^{-6})e^{-3s}}{21s+1} & \frac{(2.25\times10^{-6})e^{-4s}}{15s+1} \\ \frac{0.0015e^{-6s}}{36s+1} & \frac{0.0012e^{-5s}}{32s+1} & \frac{0.0009e^{-4.5s}}{28s+1} & \frac{0.99e^{-7.5s}}{22s+1} & \frac{-530e^{-7s}}{29s+1} & \frac{(2.29\times10^{-6})e^{-6s}}{19s+1} & \frac{(1.98\times10^{-6})e^{-4s}}{12s+1} \end{pmatrix} \end{array} \tag{12}$$

$$\mathbf{\Lambda} = \begin{array}{c} \\ y_1 \\ y_2 \\ y_3 \\ y_4 \end{array} \begin{array}{c} \begin{array}{cccc} u_1 & u_2 & u_3 & u_5 \end{array} \\ \begin{pmatrix} 0.034 & -0.035 & 0.076 & \underline{0.923} \\ \underline{1.064} & -0.001 & -0.14 & 0.076 \\ -0.184 & \underline{1.232} & 0.036 & -0.084 \\ 0.085 & -0.196 & \underline{1.026} & 0.083 \end{pmatrix} \end{array} \tag{13}$$

$$\mathbf{\Phi} = \begin{array}{c} \\ y_1 \\ y_2 \\ y_3 \\ y_4 \end{array} \begin{array}{c} \begin{array}{cccc} u_1 & u_2 & u_3 & u_4 \end{array} \\ \begin{pmatrix} 0.037 & -0.025 & 0.046 & \underline{1.033} \\ \underline{1.002} & -0.003 & -0.019 & -0.018 \\ -0.119 & \underline{1.113} & 0.054 & -0.048 \\ 0.078 & -0.084 & \underline{0972} & 0.0335 \end{pmatrix} \end{array} \tag{14}$$

$$\mathbf{\Lambda} = \begin{array}{c} \\ y_1 \\ y_2 \\ y_3 \\ y_4 \end{array} \begin{array}{c} \begin{array}{cccc} u_1 & u_2 & u_3 & u_7 \end{array} \\ \begin{pmatrix} 0.015 & 0.002 & 0.023 & \underline{0.958} \\ \underline{1.04} & -0.043 & -0.078 & 0.081 \\ -0.098 & \underline{1.159} & 0.058 & -0.119 \\ 0.042 & -0.118 & \underline{0.996} & 0.079 \end{pmatrix} \end{array} \tag{15}$$

$$\mathbf{\Phi} = \begin{array}{c} \\ y_1 \\ y_2 \\ y_3 \\ y_4 \end{array} \begin{array}{c} \begin{array}{cccc} u_1 & u_2 & u_3 & u_4 \end{array} \\ \begin{pmatrix} 0.023 & -0.021 & 0.027 & \underline{0.928} \\ \underline{1.03} & -0.104 & -0.011 & 0.085 \\ -0.054 & \underline{1.082} & 0.072 & -0.101 \\ 0.0001 & -0.0006 & \underline{0.911} & 0.087 \end{pmatrix} \end{array} \tag{16}$$

ACKNOWLEDGMENT

Technical support from Shiraz refinery, Shiraz, Iran is gratefully acknowledged.

REFERENCES

[1]S. Motlaghi, F. Jalali, M. N. Ahmadabadi, "An expert system design for a crude oil distillation column with the neural networks model and the process optimization using genetic algorithm framework," *Expert Systems with Applications*, Vol. 35, pp. 1540-1545, 2008.

[2]L. C. k. Liau, T. C. k. Yang, M. t. Tsai, "Expert system of a crude oil distillation unit for process optimization using neural networks," *Expert Systems with Applications*, Vol. 26, pp. 247-255, 2004.

[3]K. R. Muske, "Estimating the economic benefit from improved process control," *Industrial & Engineering Chemistry Research*, Vol. 42, pp. 4535-4544, 2003.

[4]A. K. Sedigh, B. Moaveni, "Control configuration selection for multivariable plants," *Springer*, 2009.

[5]F. Osuolale, J. Zhang, "Distillation Control Structure Selection for Energy-Efficient Operations," *Chemical Engineering & Technology*, Vol. 38, pp. 907-916, 2015.

[6]S. Skogestad, P. Lundstrøm, E. W. Jacobsen, "Selecting the best distillation control configuration," *AIChE Journal*, Vol. 36, pp. 753-764, 1990.

[7]D. Jones, D. Bhattacharyya, R. Turton, S. E. Zitney, "Plantwide control system design: Primary controlled variable selection," *Computers & Chemical Engineering*, Vol. 71, pp. 220-234, 2014.

[8]X. Luan, Q. Chen, F. Liu, "Interaction measurement for complex multivariable models with various reference inputs based on RNGA," *Control Conference (ASCC), 11th Asian. IEEE*, pp. 2411-2416, 2017.

[9]P. H. Naik, D. A. Kumar, K. Anjaneyulu, "Loop Interaction and Its Influence in Multivariable Process Control," *Emerging Trends in Electrical, Communications and Information Technologies, Springer*, pp. 361-368, 2017.

[10]R. Agustriyanto, J. Zhang, "Closed-loop simulation of decentralized control using RGA for uncertain binary distillation column," *IOP Conference Series: Materials Science and Engineering. IOP Publishing*, pp. 012012, 2017.

[11]E. Bristol, "On a new measure of interaction for multivariable process control," *IEEE Transactions on Automatic Control*, Vol. 11, pp. 133-134, 1966.

[12]V. Kariwala, S. Skogestad, J. F. Forbes, "Relative gain array for norm-bounded uncertain systems," *Industrial & Engineering Chemistry Research*, Vol. 45, pp. 1751-1757, 2006.

[13]A. K. Sedigh, B. Moaveni, "Relative gain array analysis of uncertain multivariable plants," *Proceeding of the 7th European Control Conference, Cambridge, UK*, 2003.

[14]V. C. Machado, D. Gabriel, J. Lafuente, J. A. Baeza, "Cost and effluent quality controllers design based on the relative gain array for a nutrient removal WWTP," *Water Research*, Vol. 43, pp. 5129-5141, 2009.

[15]G. Pandimadevi, P. Indumathi, V. Selvakumar, "Design of Controllers for a Fluidized Catalytic Cracking Process," *Chemical Engineering Research and Design*, Vol. 88, pp. 875-880, 2010.

[16]C. Bo, R. Zhang, C. Zhang, J. Tang, X. Qiao, F. Gao, "Comparison of Two Types of Control Structures for Benzene Chlorine Reactive Distillation Systems," *Chinese Journal of Chemical Engineering*, Vol. 22, pp. 837-841, 2014.

[17]N. Chatrattanawet, S. Skogestad, A. Arpornwichanop, "Control structure design and dynamic modelling for a solid oxide fuel cell with direct internal reforming of methane," *Chemical Engineering Research and Design*, Vol. 98, pp. 202-211, 2015.

[18]T. M. Avoy, Y. Arkun, R. Chen, D. Robinson, P. D. Schnelle, "A new approach to defining a dynamic relative gain," *Control Engineering Practice*, Vol. 11, pp. 907-914, 2003.

[19]Q. Xiong, W. J. Cai, M. J. He, "A practical loop pairing criterion for multivariable processes," *Journal of Process Control*, Vol. 15, pp. 741-747, 2005.

[20]M. J. He, W. J. Cai, W. Ni, L. H. Xie, "RNGA based control system configuration for multivariable processes, " *Journal of Process Control*, Vol. 19, pp. 1036-1042, 2009.

[21]A. Drews, "ASTM manual on hydrocarbon analysis," *Standard Test Method D3238-90, Philadelphia*, 1989.

[22]D. J. Dave, M. Z. Dabhiya, S. Satyadev, S. Ganguly, D. N. Saraf, "Online tuning of a steady state crude distillation unit model for real time applications," *Journal of Process Control*, Vol. 13, pp. 267-282, 2003.

[23]C. D. Holland, "Fundamentals of multicomponent distillation," *McGraw-Hill, New York*, 1981.

[24]V. Kumar, A. Sharma, I. R. Chowdhury, S. Ganguly, D. N. Saraf, "A crude distillation unit model suitable for online applications," *Fuel Processing Technology*, Vol. 73, pp. 1-21, 2001.

[25]B. D. Tyreus, W. L. Luyben, "Tuning PI controllers for integrator/dead time processes," *Industrial & Engineering Chemistry Research*, Vol. 31, pp. 2625-2628, 1992.

[26]W. L. Luyben, "Distillation design and control using Aspen simulation," *John Wiley & Sons*, 2013.

[27]L. Yunhui, L. Hongbo, C. Wenjian, J. Zhiping, J. Lei, S. Ruifu, "Control configuration selection based on RNGA for non-square multivariable processes," *Control Conference (CCC), 31st Chinese, IEEE*, pp. 4722-4727, 2012.



Mir Mohammad Khalilipour received the bachelors degree in chemical engineering from Quchan University in 2004 and the masters and Ph.D. degrees in chemical engineering process design from the University of Sistan and Baluchistan, Iran, in 2008 and 2016, respectively. He was involved in safety management industrial projects for many Iranian oil and gas refineries from 2008 to 2011. He is currently an Assistant Professor with the Chemical Engineering Department, University of Sistan and Baluchestan. His research interests are the chemical safety, control and process simulation specifically focusing on practical interesting of control, and soft sensors in chemical processes.



Farhad Shahraki received the B.S. degree in chemical engineering from the University of Sistan and Baluchestan, Zahedan, Iran, in 1989, the M.S. degree in chemical engineering from Tarbiat Modares University, Tehran, Iran, in 1992, and the Ph.D. degree in chemical engineering from The University of Manchester, Manchester, U.K., in 2001. He is currently a Professor of Chemical Engineering with the University of Sistan and Baluchestan. His research interests include process integration, process modeling, and optimization.



Jafar Sadeghi received the B.S. degree in chemical engineering from the Isfahan University of Technology, Isfahan, Iran, in 1991, the M.S. degree in chemical engineering from the Sharif University of Technology, Tehran, Iran, in 1995, and the Ph.D. degree in chemical engineering from the University of Lancaster, U.K., in 2007. He is currently an Associate Professor with the University of Sistan and Baluchestan, Zahedan, Iran. His research interests cover process modeling and simulation, process control, process identification, process intensification, automation, and instrumentation.



Kiyanoosh Razzaghi received the B.S. degree in chemical engineering from the Iran University of Science and Technology, Tehran, Iran, in 2002, the M.S. and Ph.D. degrees in chemical engineering from the University of Sistan and Baluchestan, Zahedan, Iran, in 2005, and 2010. He is currently an Assistant Professor with the University of Sistan and Baluchestan, Zahedan, Iran. His research interests cover process modeling and simulation, process control and optimization, low pressure drop static mixers.